

# Molecular emission lines from simulations of AGN-driven molecular outflows

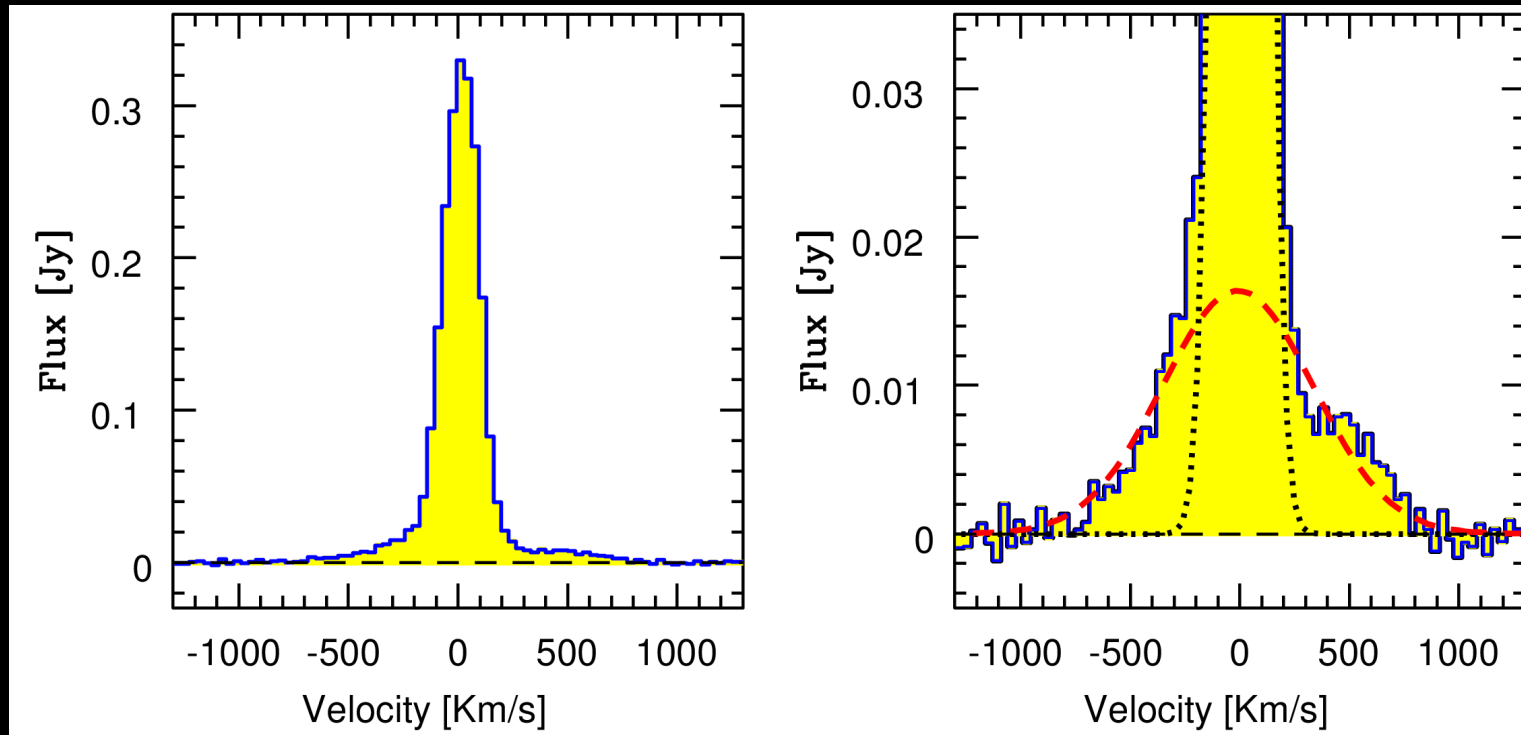
Alex Richings, Claude-André Faucher-Giguère  
CIERA, Northwestern University

16<sup>th</sup> March 2018

# Introduction

## Observations of fast molecular outflows

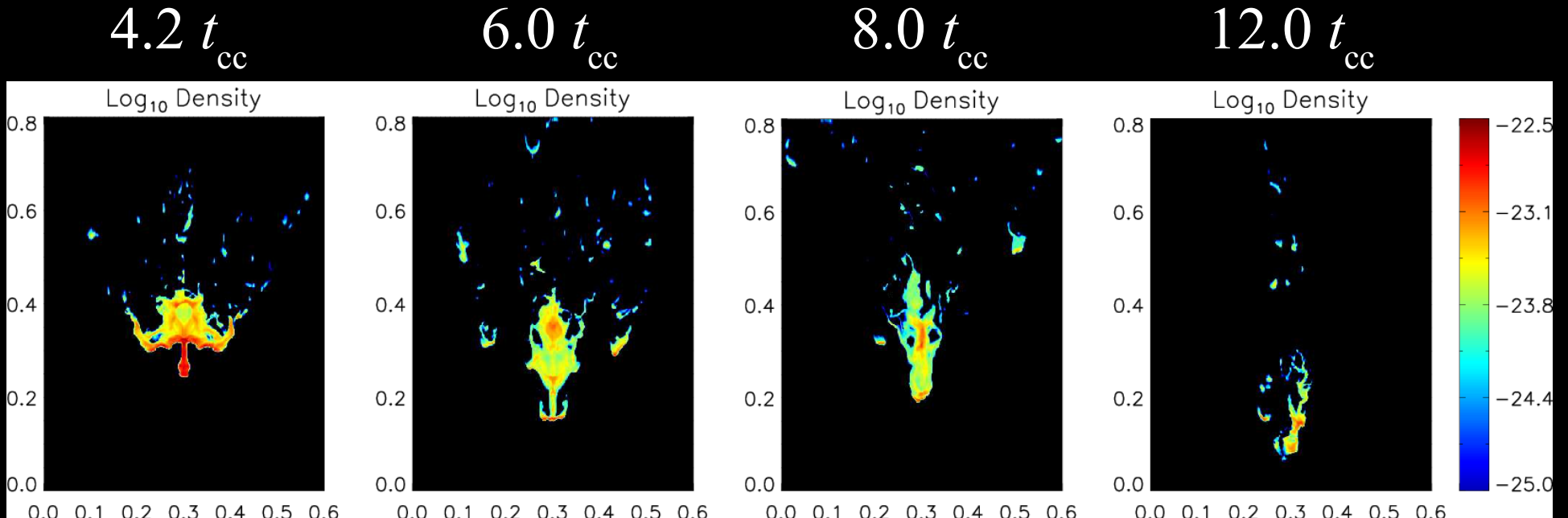
### CO 1-0 line in Mrk 231



Feruglio et al. (2010)

# Introduction

## Acceleration of cold clouds

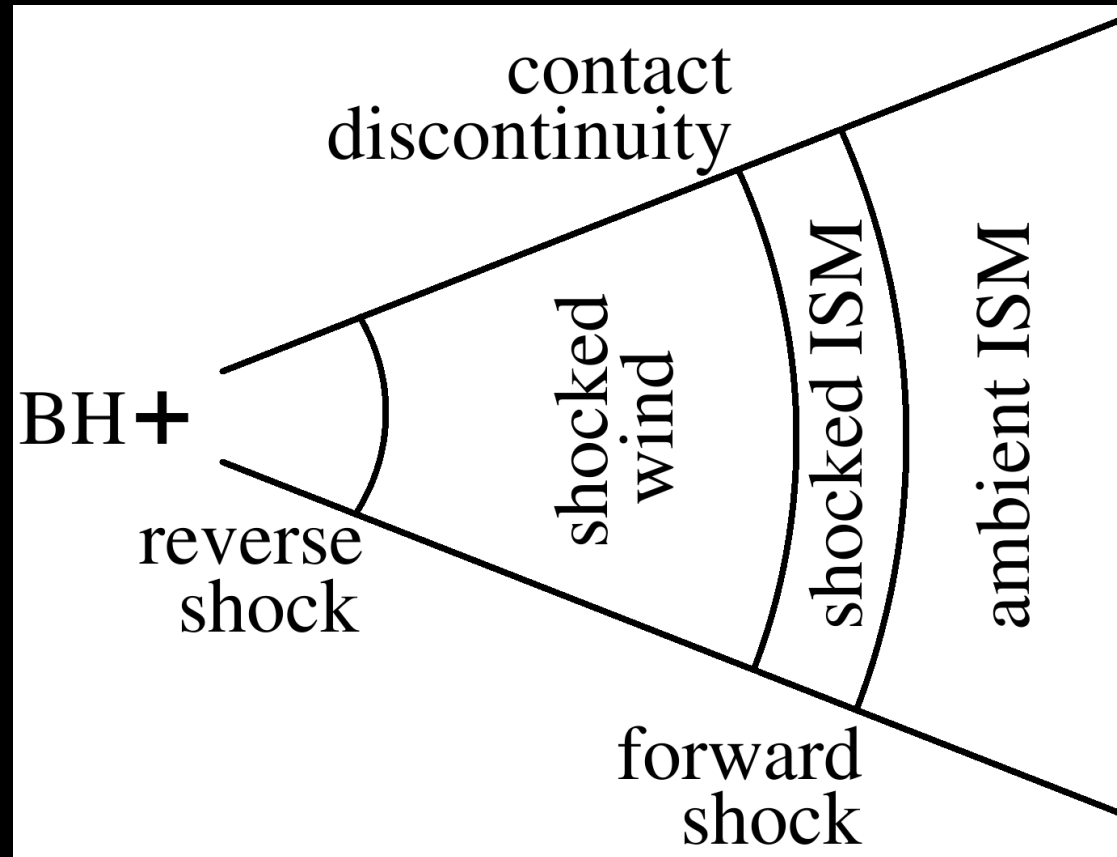


Scannapieco & Brüggen (2015)

# Introduction

## In-situ molecule formation

### An energy-driven AGN wind



# Simulations

- 3D simulations of an isotropic AGN wind.
- 1.6-5.0 kpc box, periodic boundary conditions.
- Inject wind particles, initial  $v = 30,000 \text{ km s}^{-1}$ ,  
 $dP/dt = L_{\text{AGN}}/c$ .

# Simulations

- 3D simulations of an isotropic AGN wind.
- 1.6-5.0 kpc box, periodic boundary conditions.
- Inject wind particles, initial  $v = 30,000 \text{ km s}^{-1}$ ,  
 $dP/dt = L_{\text{AGN}}/c$ .

## Chemistry

- Evolve time-dependent chemistry of 157 species, including 20 molecules.
- Most importantly: H<sub>2</sub>, CO, OH and HCO<sup>+</sup>.
- We assume a Milky Way dust-to-metals ratio.

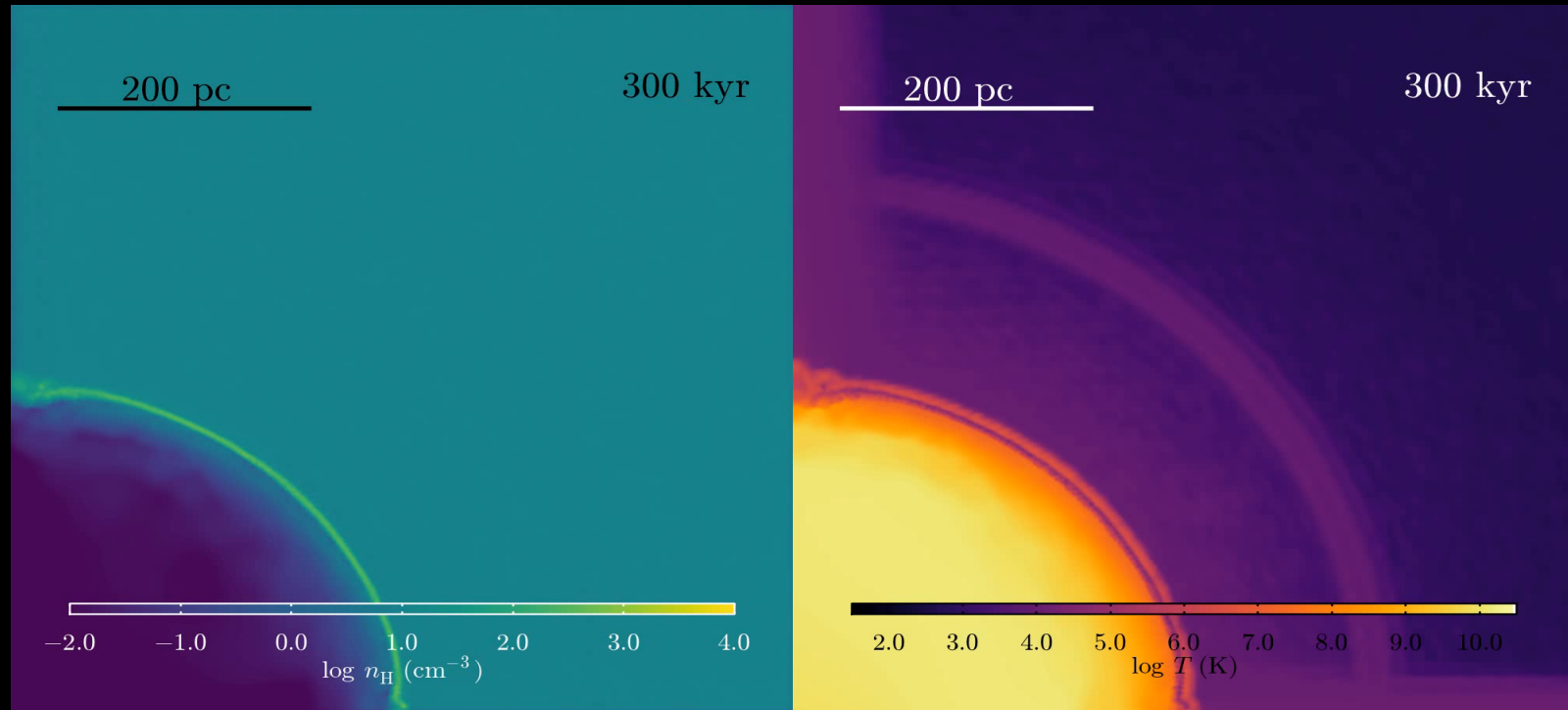
# Simulations

## Parameters

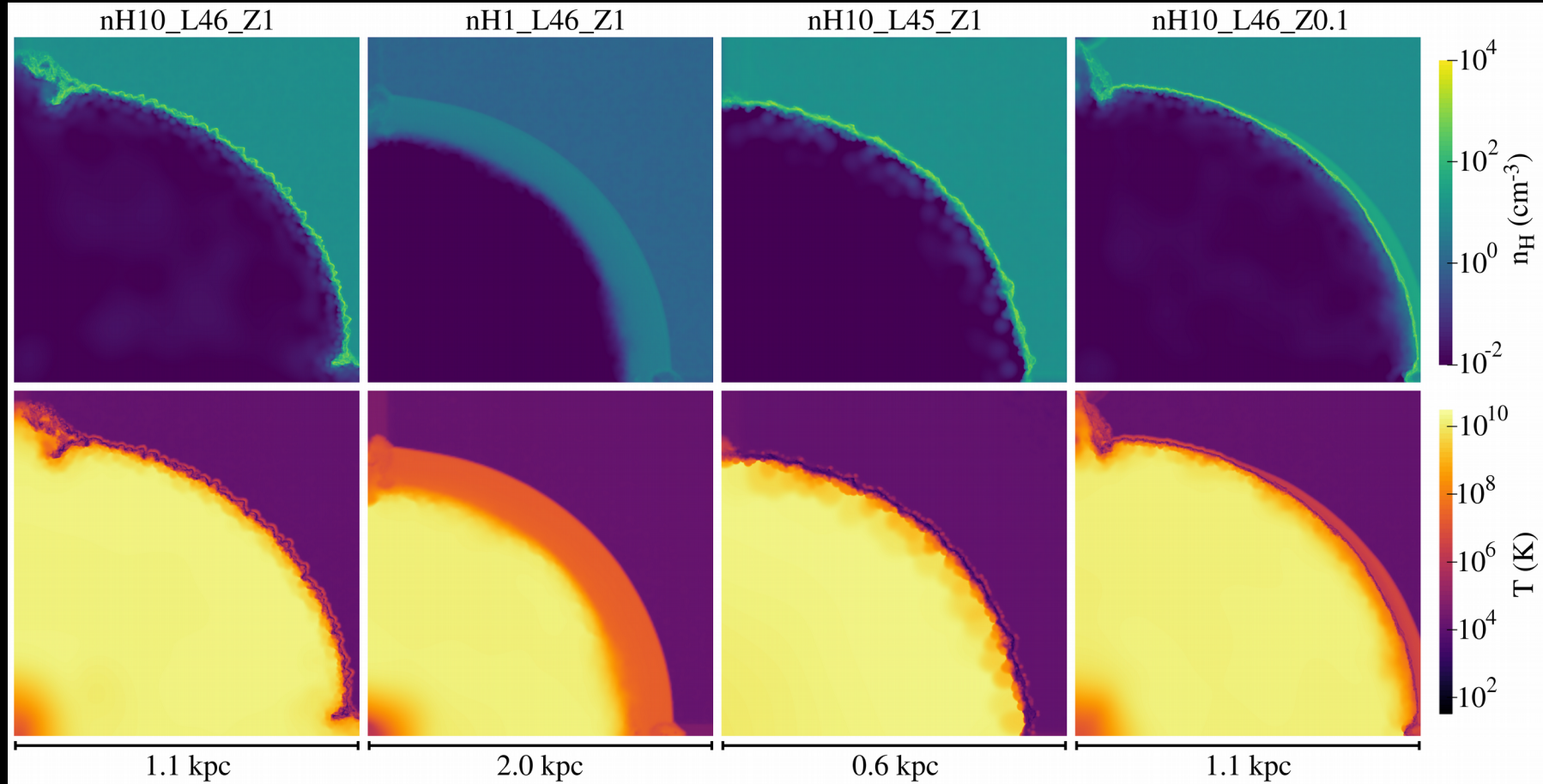
$n_{\text{H}}$ (cm $^{-3}$ )	$L_{\text{AGN}}$ (erg s $^{-1}$ )	$Z / Z_{\text{sol}}$
10	$10^{46}$	1.0
1	$10^{46}$	1.0
10	$10^{45}$	1.0
10	$10^{46}$	0.1

# Simulations

nH10\_L45\_Z1



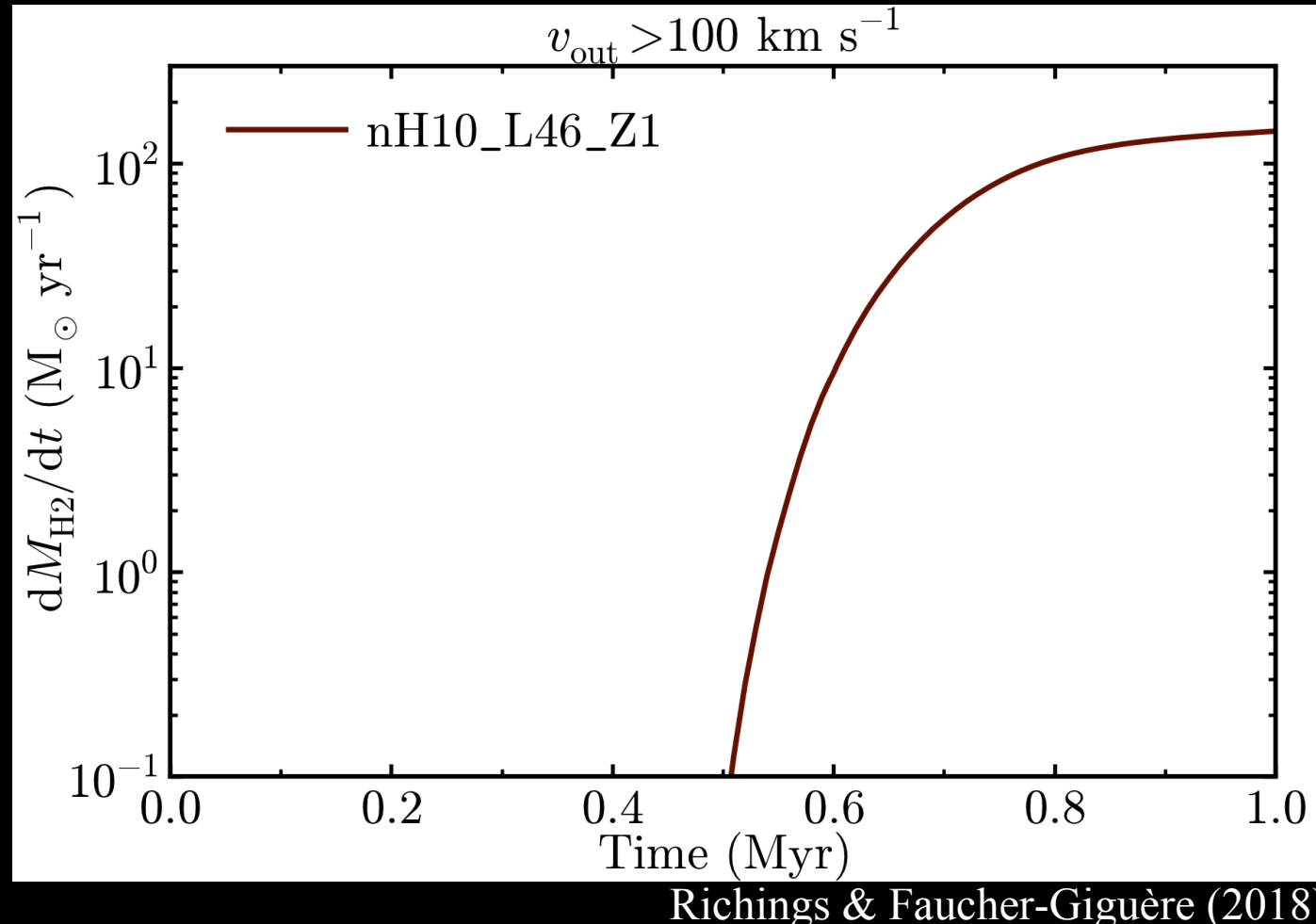
# Simulations



Richings & Faucher-Giguère (2018)

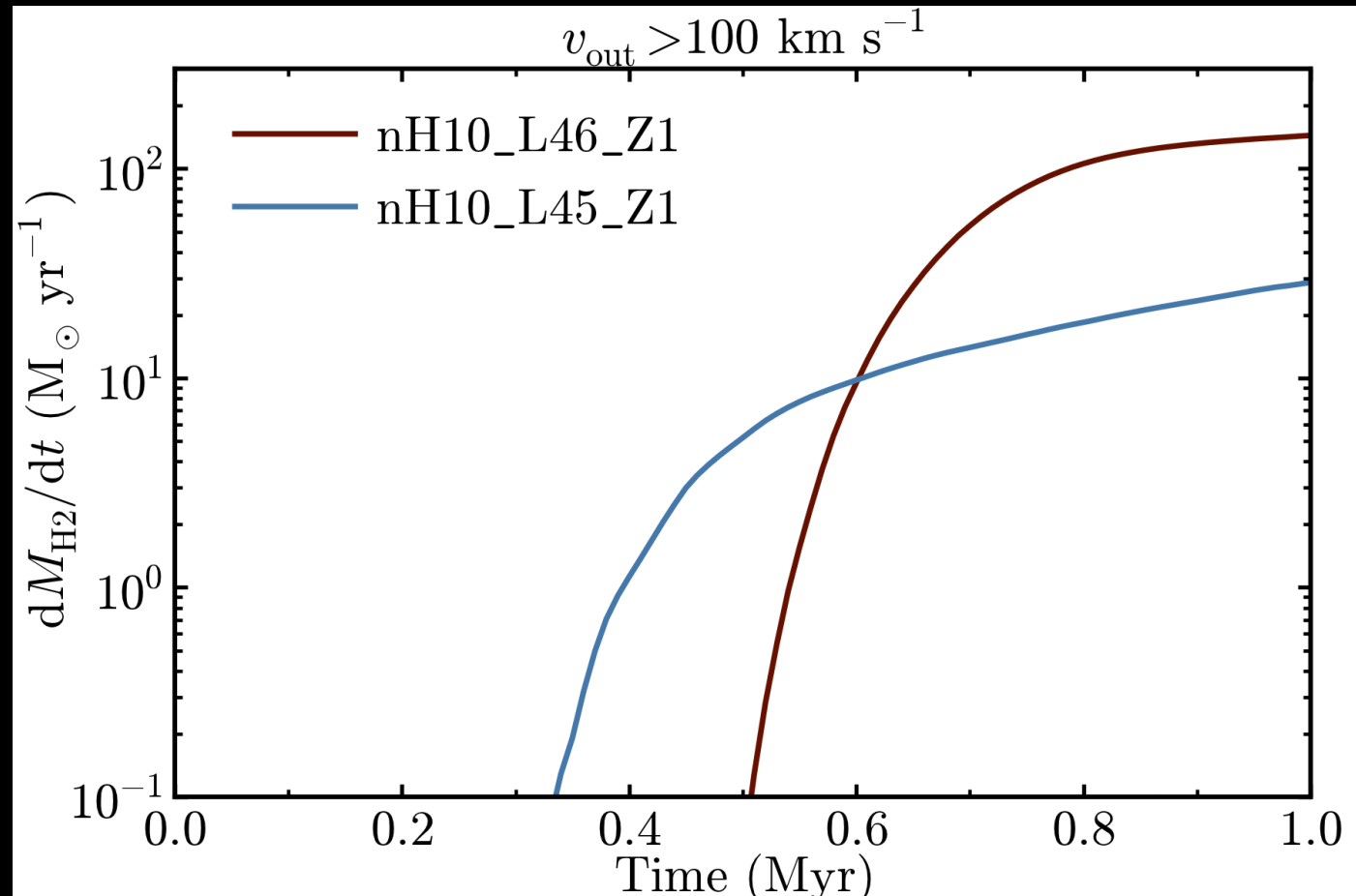
# Simulations

## H<sub>2</sub> outflow rates



# Simulations

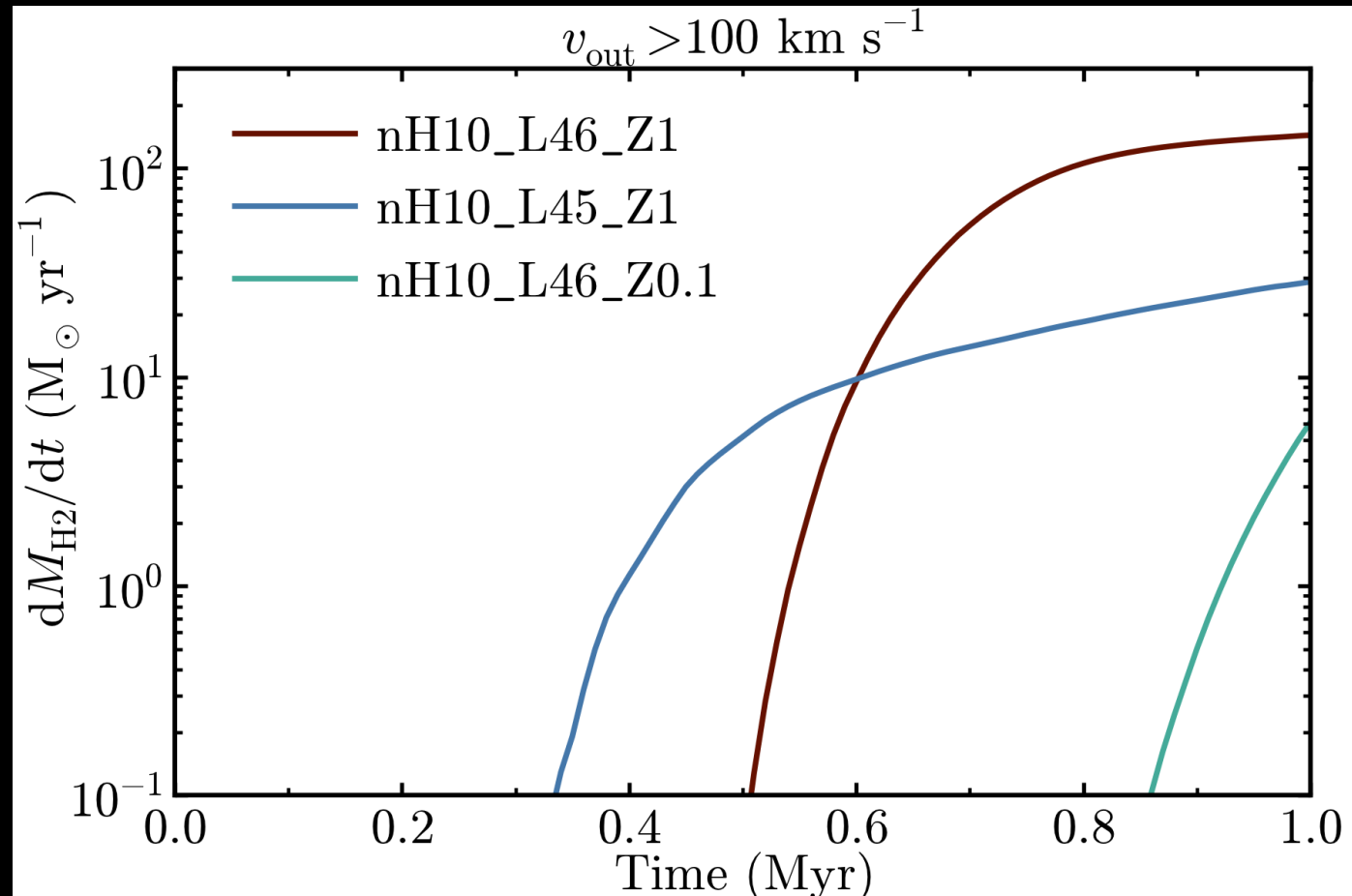
## H<sub>2</sub> outflow rates



Richings & Faucher-Giguère (2018)

# Simulations

## H<sub>2</sub> outflow rates



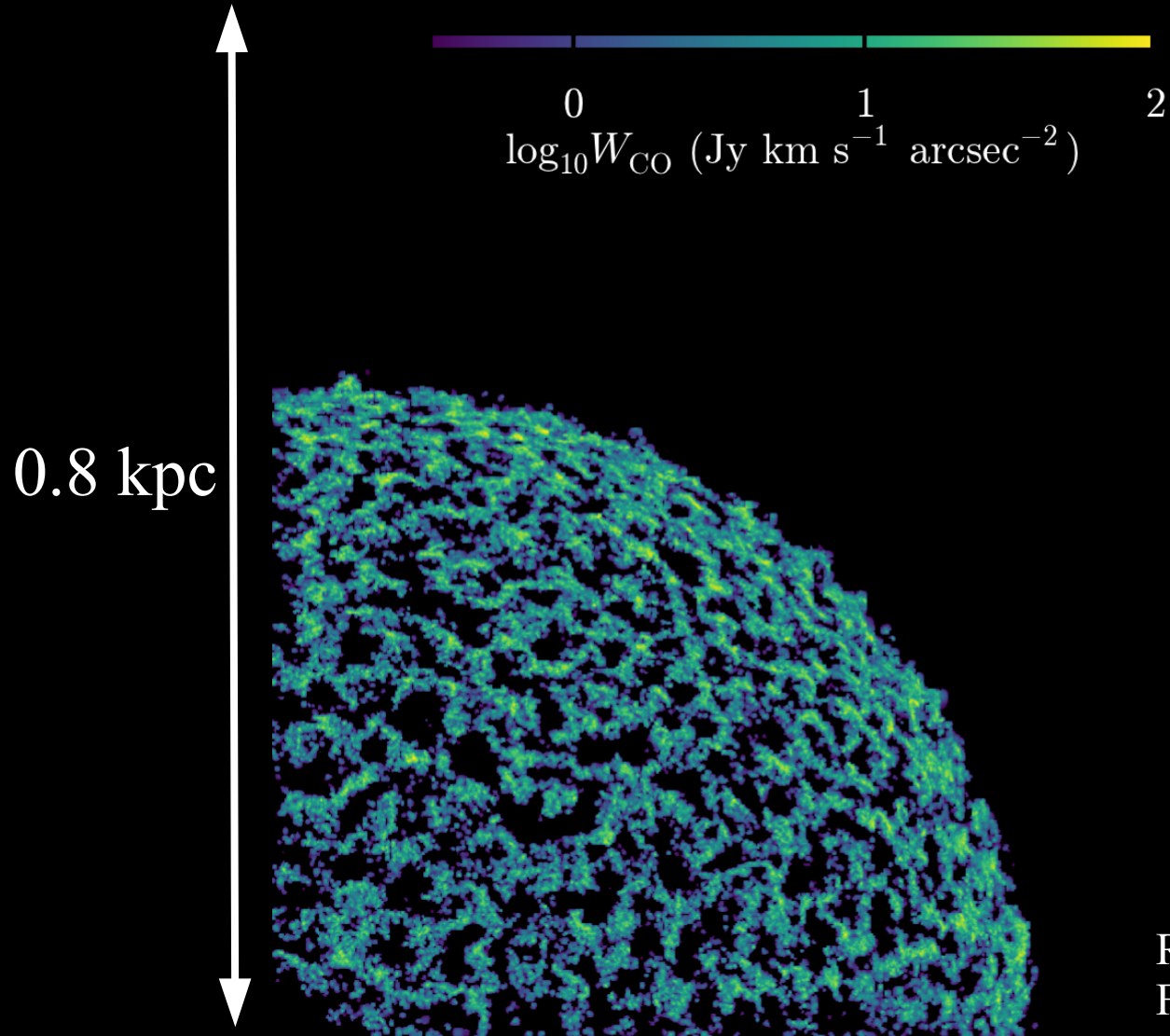
Richings & Faucher-Giguère (2018)

# Molecular Emission Lines

- We use the Monte Carlo radiative transfer code RADMC-3D (Dullemond et al. 2012).
- Interpolate particles from the simulations onto an AMR grid, with maximum spatial resolution of 0.07 pc.
- Use non-equilibrium chemical abundances from the simulations.
- CO emission, warm (few hundred K) H<sub>2</sub> emission, and OH absorption.

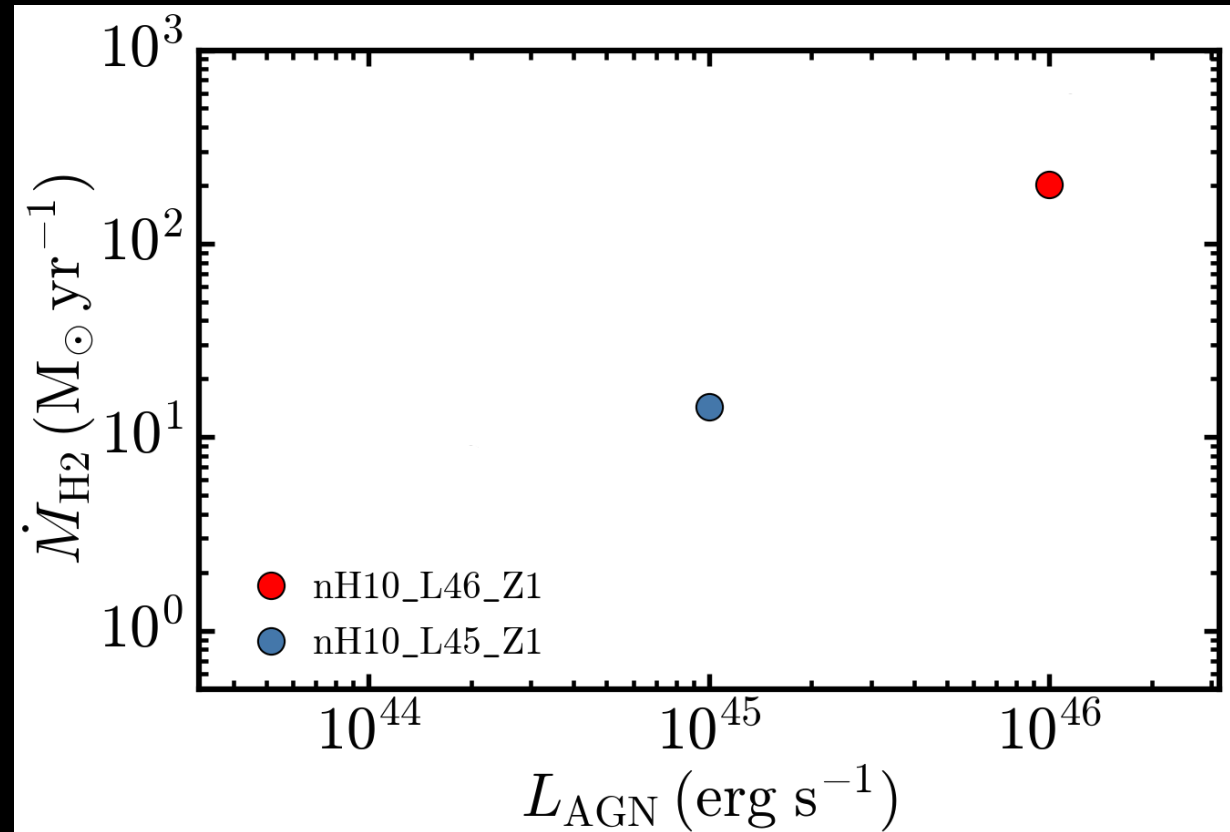
# CO 1-0 line emission

nH10\_L45\_Z1



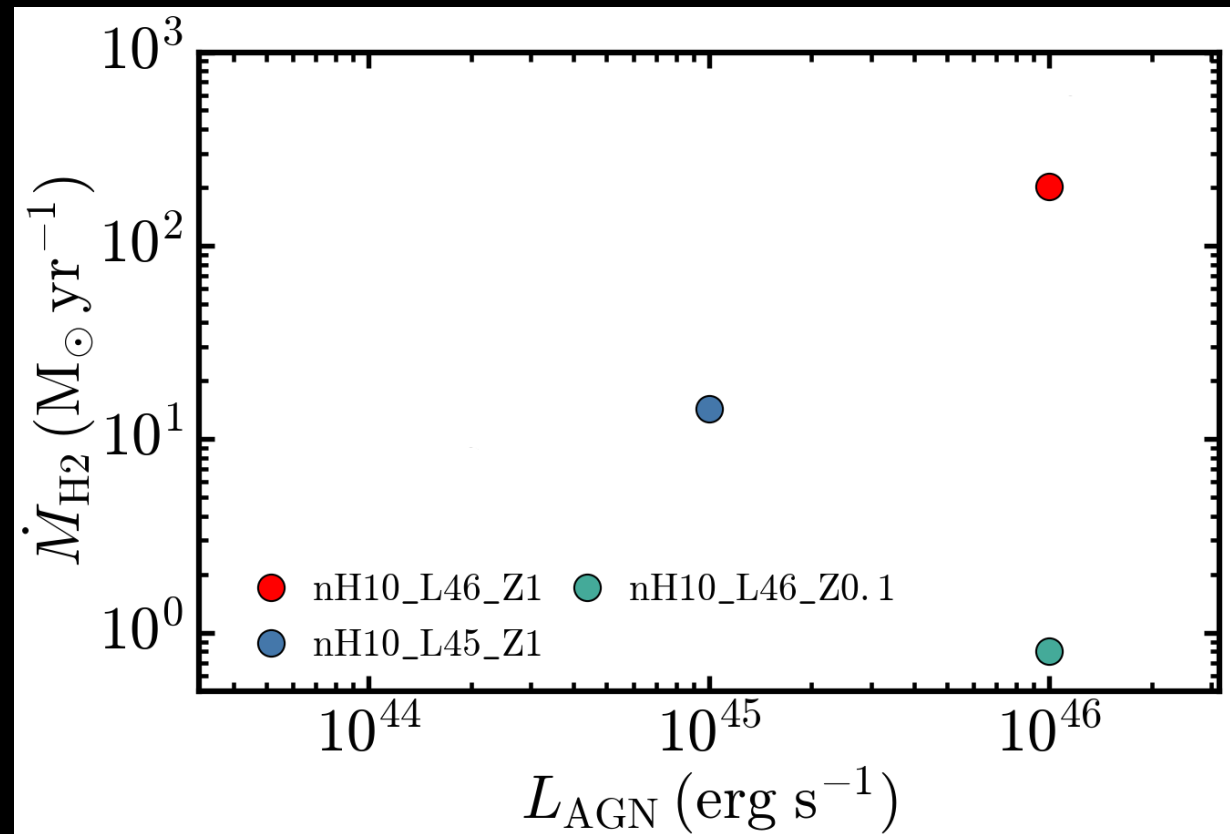
Richings &  
Faucher-Giguère (2018)

# Comparison with CO-based observations



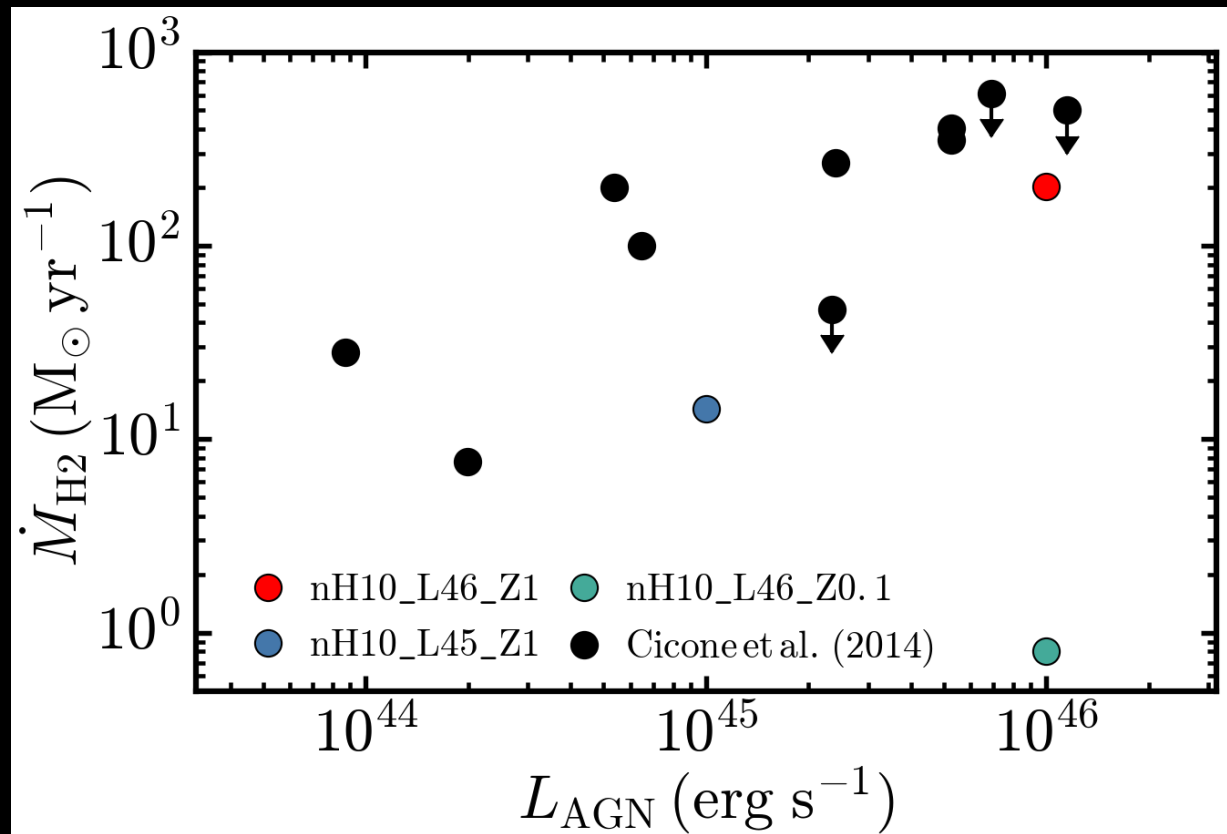
Richings & Faucher-Giguère (2018)

# Comparison with CO-based observations



Richings & Faucher-Giguère (2018)

# Comparison with CO-based observations



Richings & Faucher-Giguère (2018)

# CO-to-H<sub>2</sub> conversion factors

Simulation	$\alpha_{\text{CO}} = M_{\text{H}_2} / L_{\text{CO}}^*$		
	(1-0)	(2-1)	(3-2)
nH10_L46_Z1	0.13	0.08	0.06
nH10_L45_Z1	0.15	0.09	0.07
nH10_L46_Z0.1	1.77	0.82	0.80

\*Units:  $M_{\text{sol}} (\text{K km s}^{-1} \text{ pc}^2)^{-1}$

# CO-to-H<sub>2</sub> conversion factors

Simulation	$\alpha_{\text{CO}} = M_{\text{H}_2} / L_{\text{CO}}^*$		
	(1-0)	(2-1)	(3-2)
nH10_L46_Z1	0.13	0.08	0.06
nH10_L45_Z1	0.15	0.09	0.07
nH10_L46_Z0.1	1.77	0.82	0.80

\*Units:  $M_{\text{sol}} (\text{K km s}^{-1} \text{ pc}^2)^{-1}$

# CO-to-H<sub>2</sub> conversion factors

Simulation	$\alpha_{\text{CO}} = M_{\text{H}_2} / L_{\text{CO}}^*$		
	(1-0)	(2-1)	(3-2)
nH10_L46_Z1	0.13	0.08	0.06
nH10_L45_Z1	0.15	0.09	0.07
nH10_L46_Z0.1	1.77	0.82	0.80

\*Units:  $M_{\text{sol}} (\text{K km s}^{-1} \text{ pc}^2)^{-1}$

# CO-to-H<sub>2</sub> conversion factors

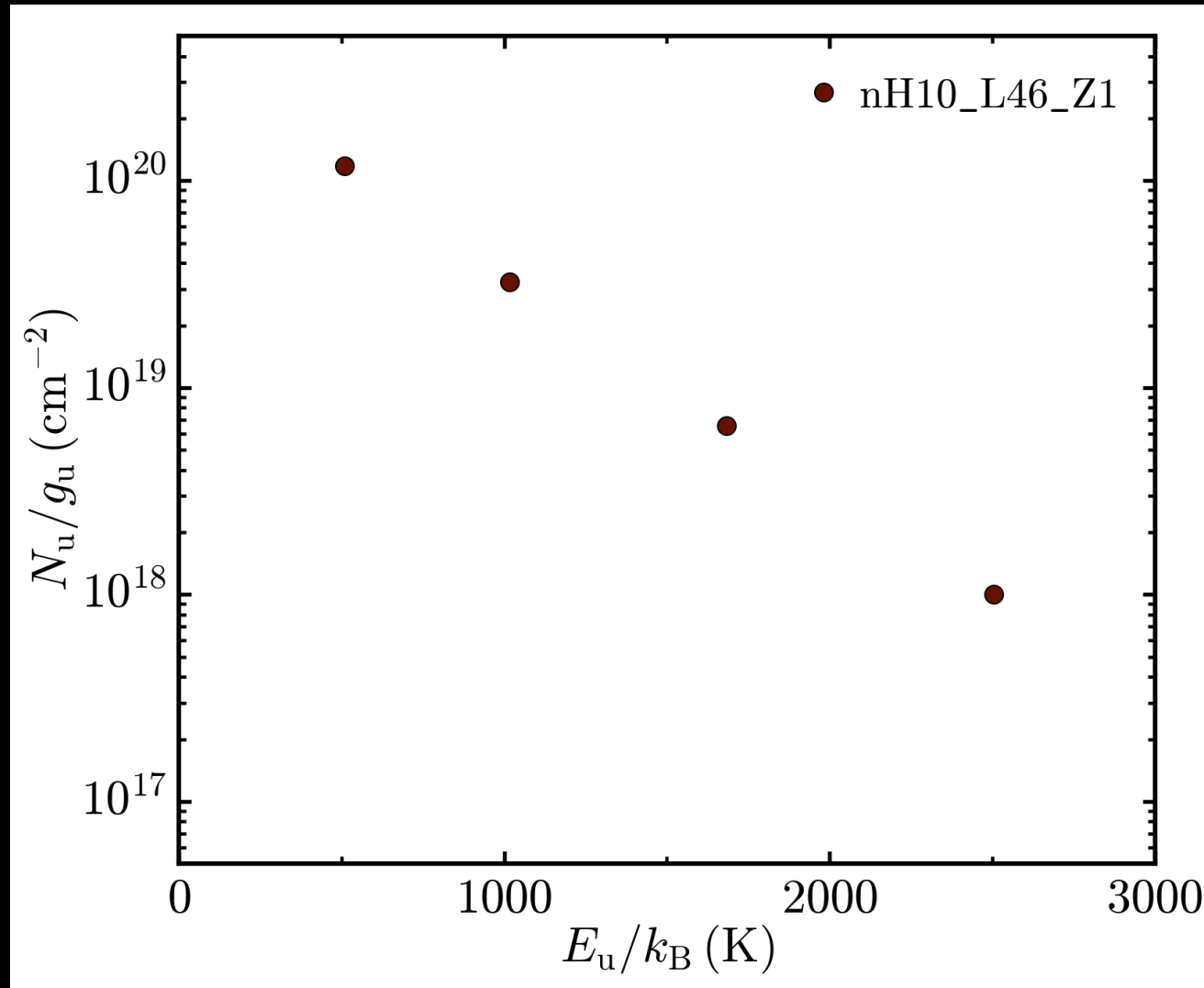
Simulation	$\alpha_{\text{CO}} = M_{\text{H}_2} / L_{\text{CO}}^*$		
	(1-0)	(2-1)	(3-2)
nH10_L46_Z1	0.13	0.08	0.06
nH10_L45_Z1	0.15	0.09	0.07
nH10_L46_Z0.1	1.77	0.82	0.80

\*Units:  $M_{\text{sol}} (\text{K km s}^{-1} \text{ pc}^2)^{-1}$

➤ Observations typically assume:

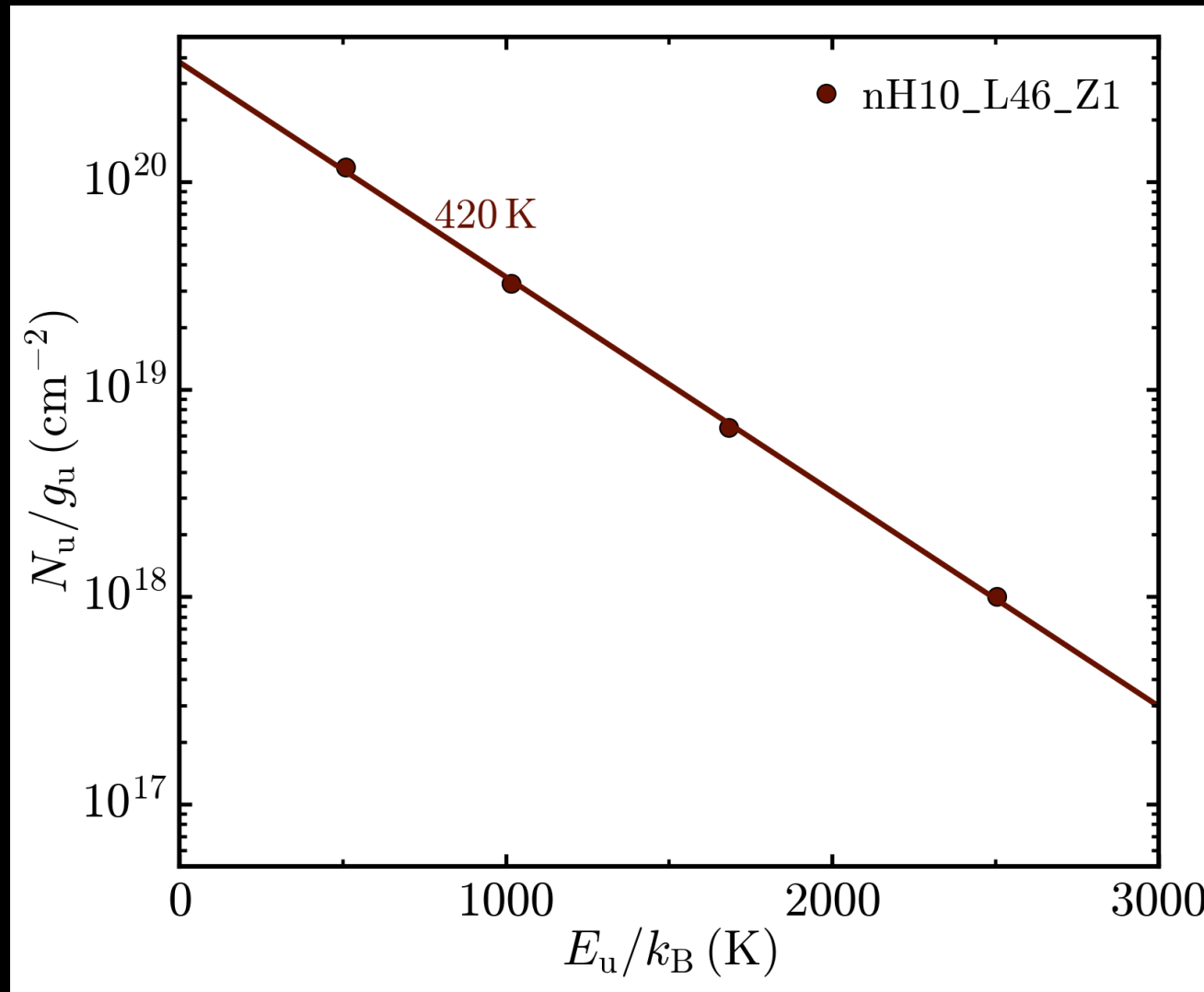
$$\alpha_{\text{CO (1-0)}} = 0.8 M_{\text{sol}} (\text{K km s}^{-1} \text{ pc}^2)^{-1}.$$

# Warm H<sub>2</sub> Emission



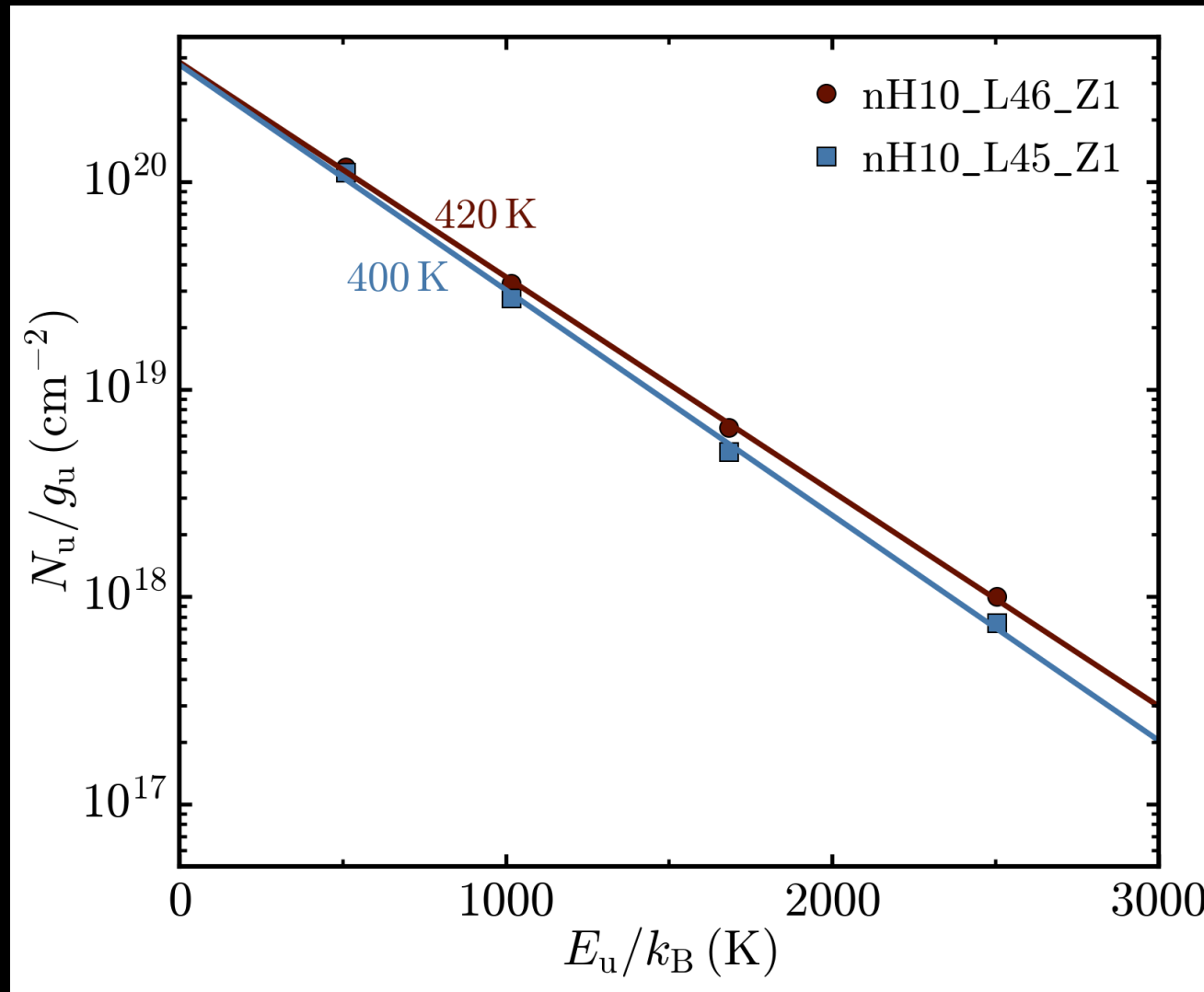
Richings & Faucher-Giguère (2018)

# Warm H<sub>2</sub> Emission



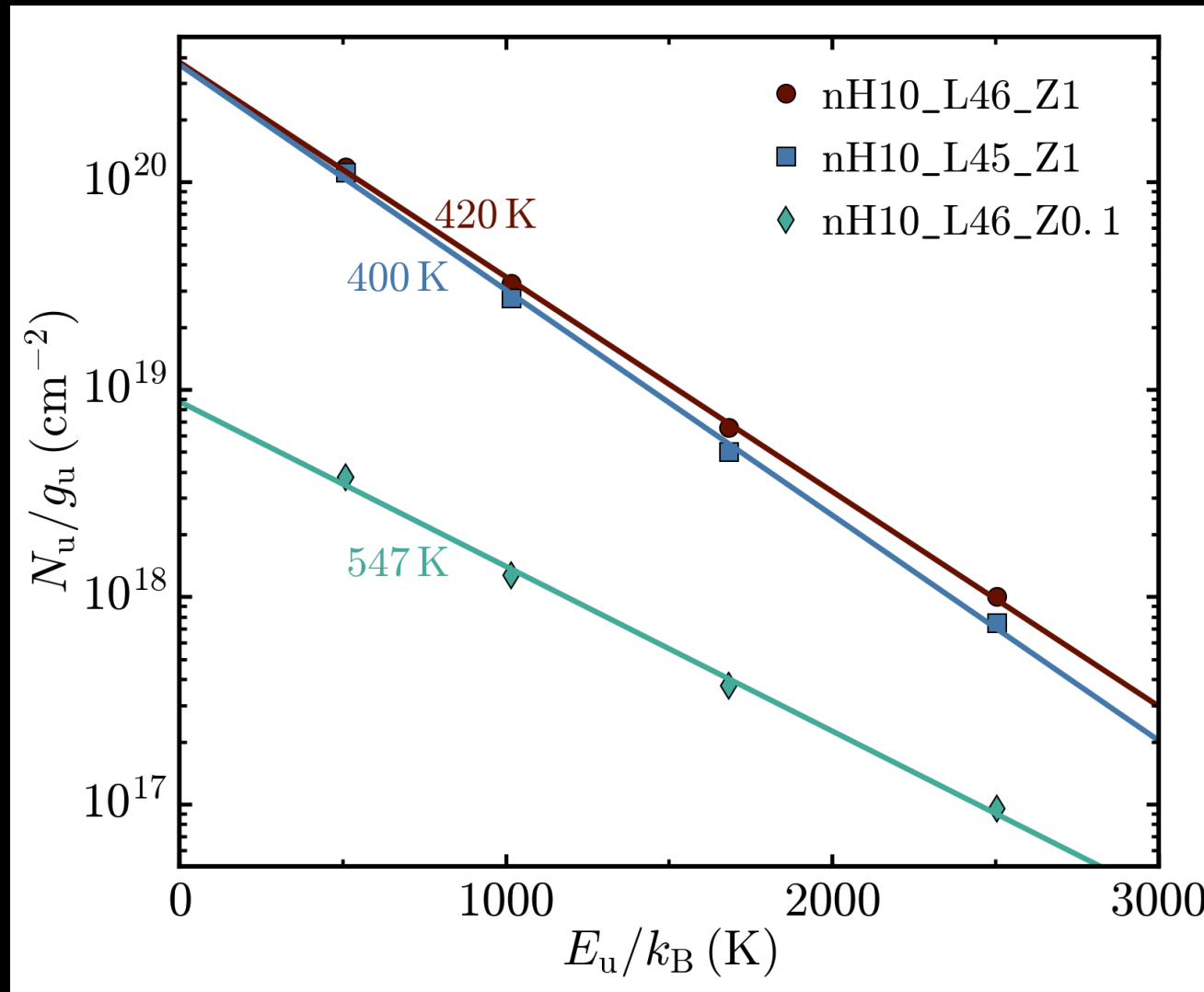
Richings & Faucher-Giguère (2018)

# Warm H<sub>2</sub> Emission



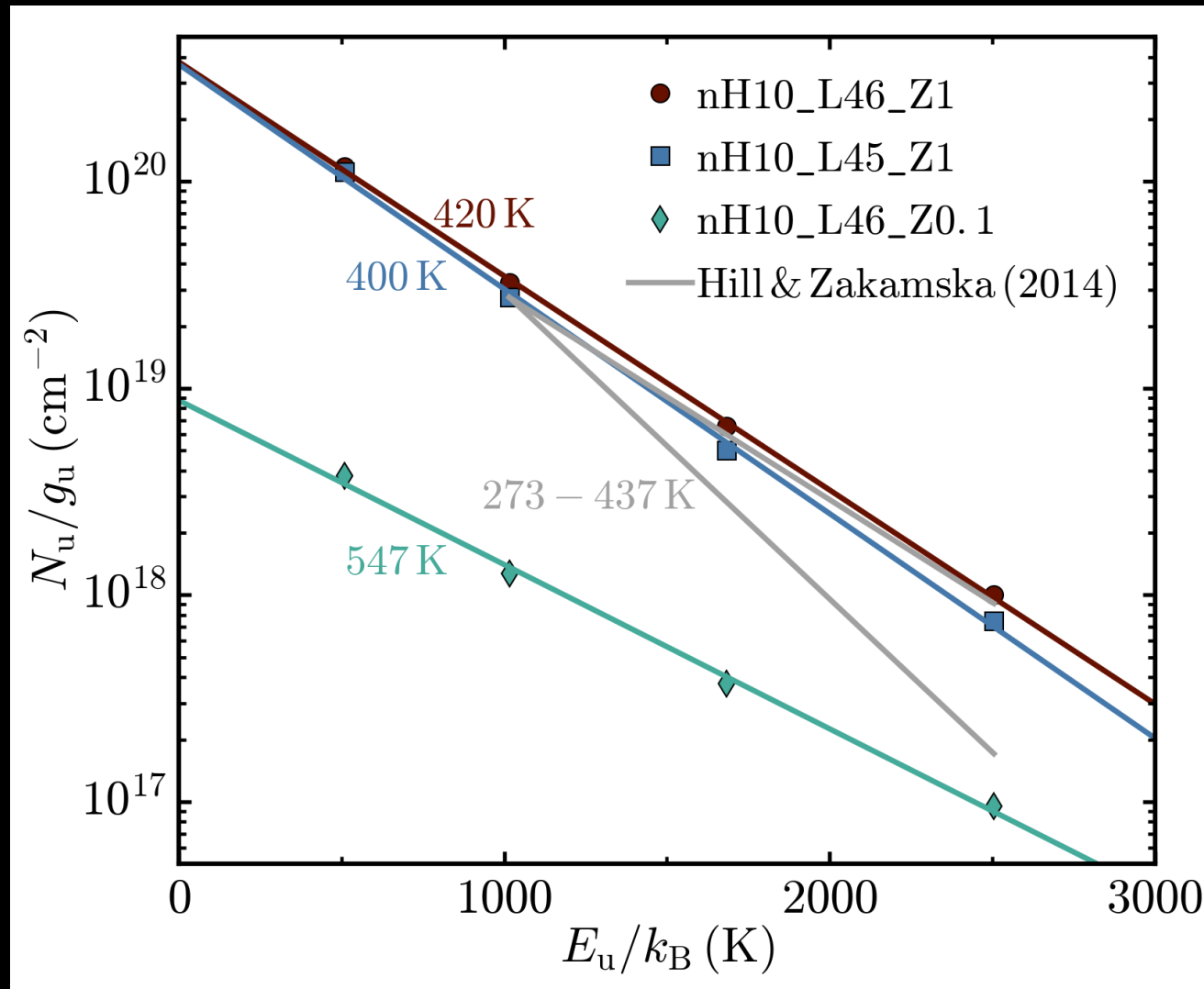
Richings & Faucher-Giguère (2018)

# Warm H<sub>2</sub> Emission



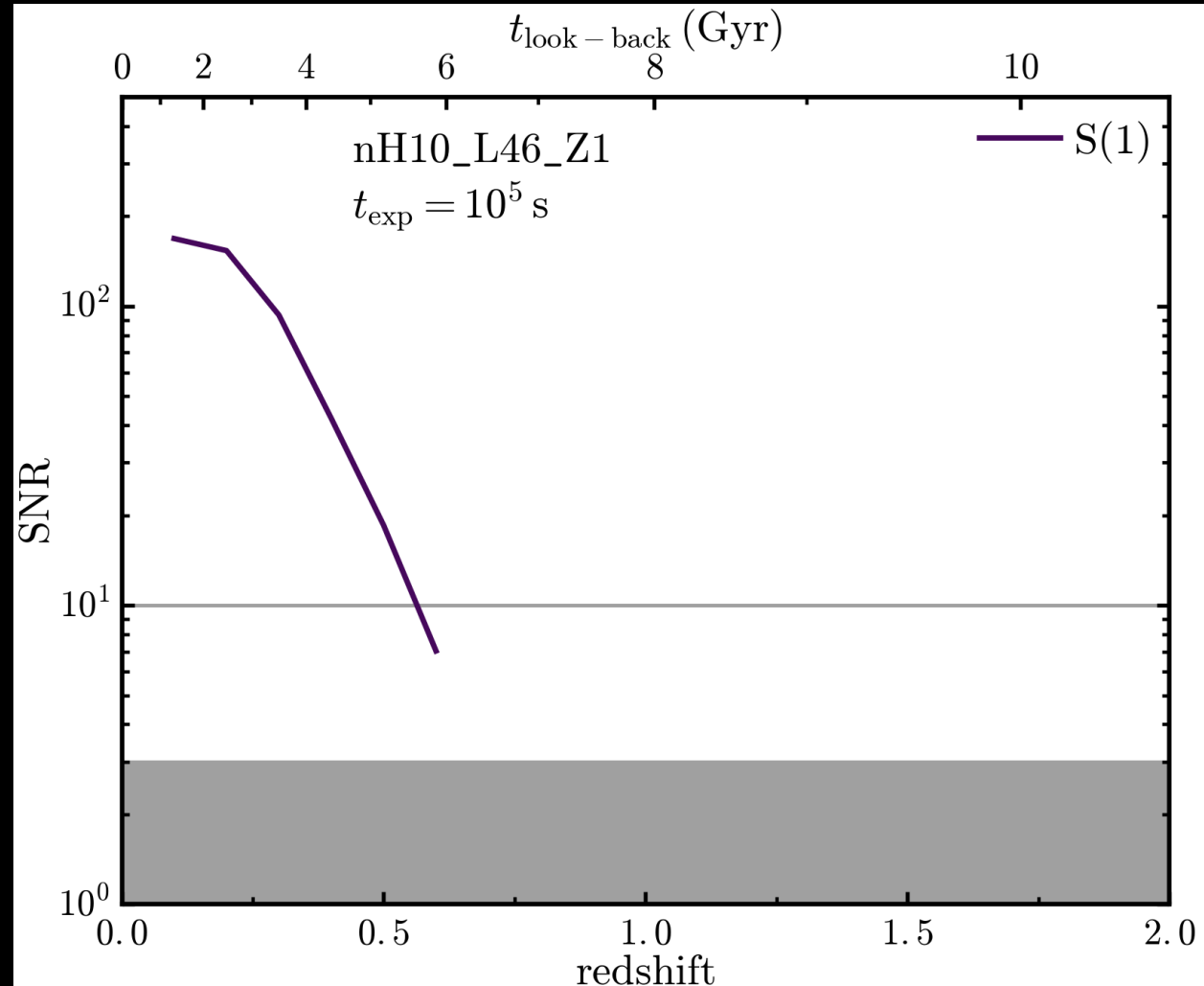
Richings & Faucher-Giguère (2018)

# Warm H<sub>2</sub> Emission



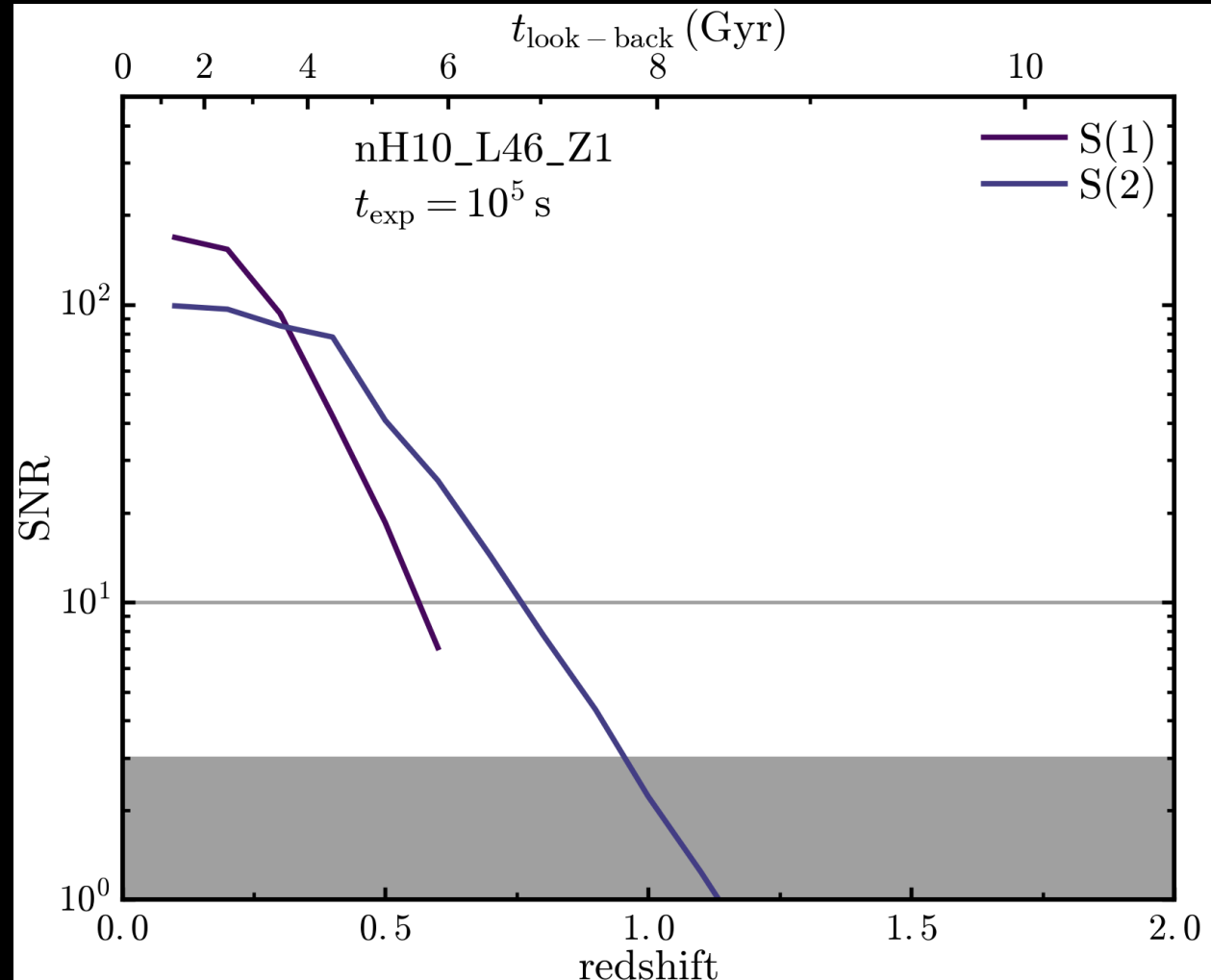
Richings & Faucher-Giguère (2018)

# Warm H<sub>2</sub> Emission JWST Predictions



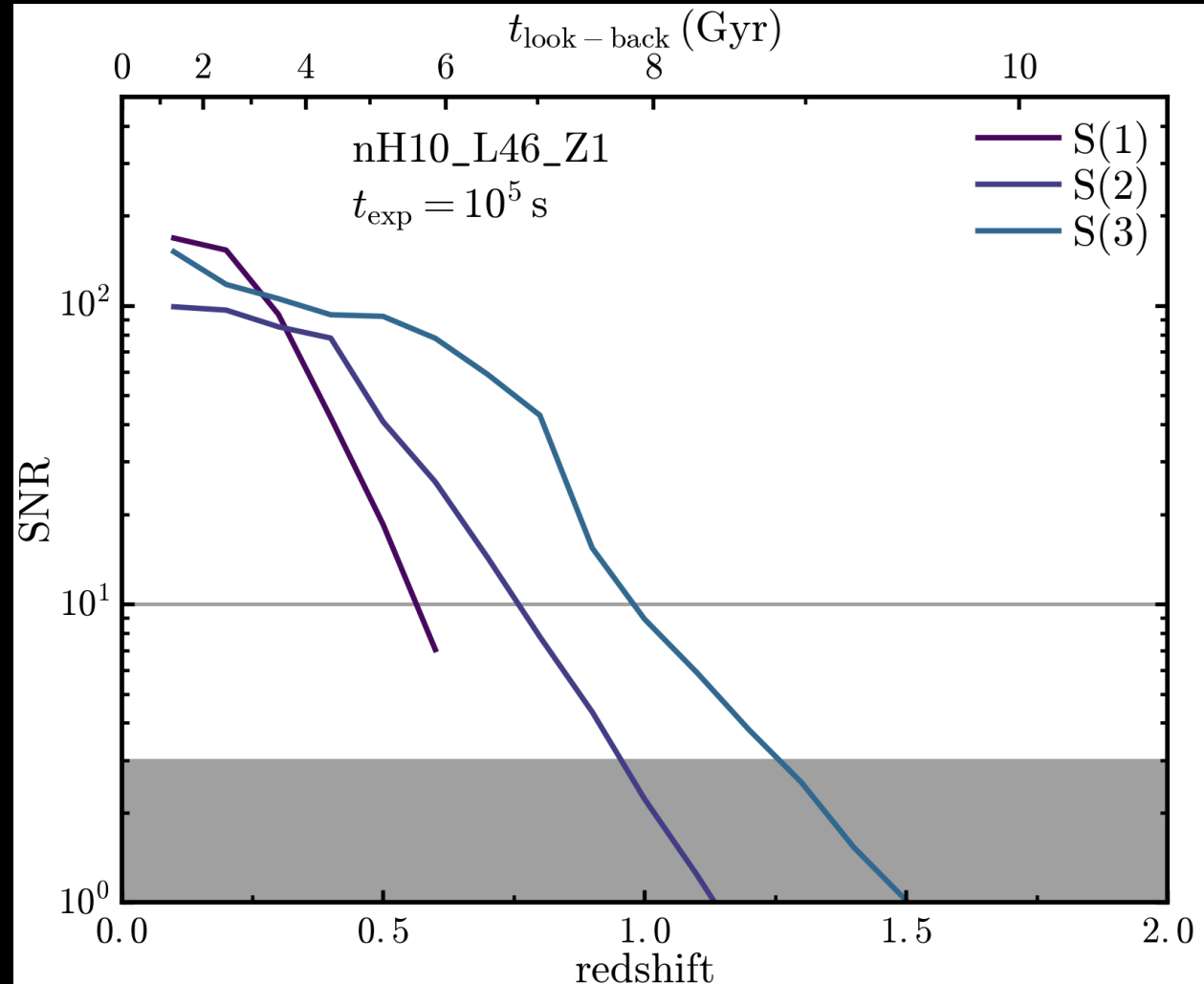
Richings & Faucher-Giguère (in prep)

# Warm H<sub>2</sub> Emission JWST Predictions



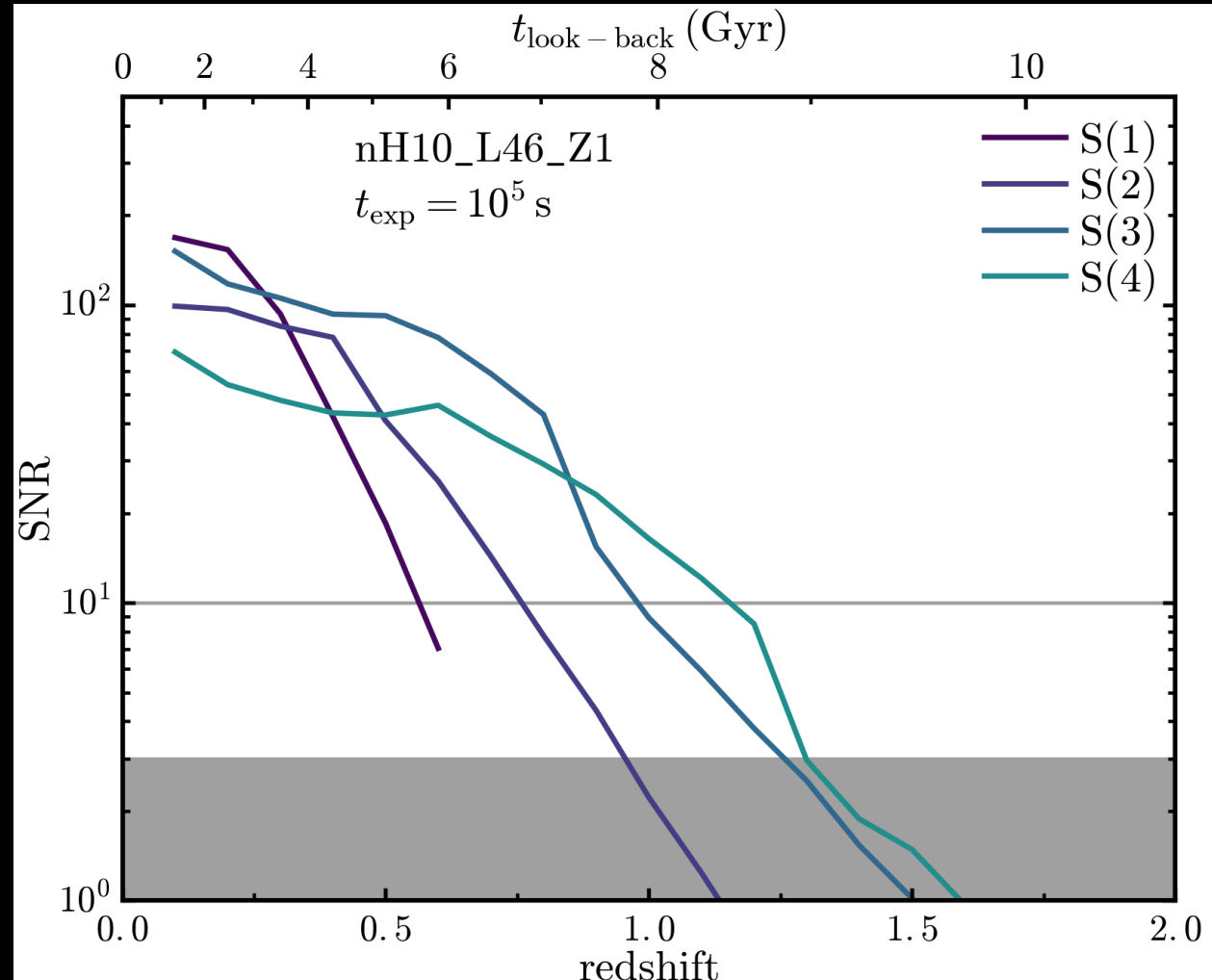
Richings & Faucher-Giguère (in prep)

# Warm H<sub>2</sub> Emission JWST Predictions



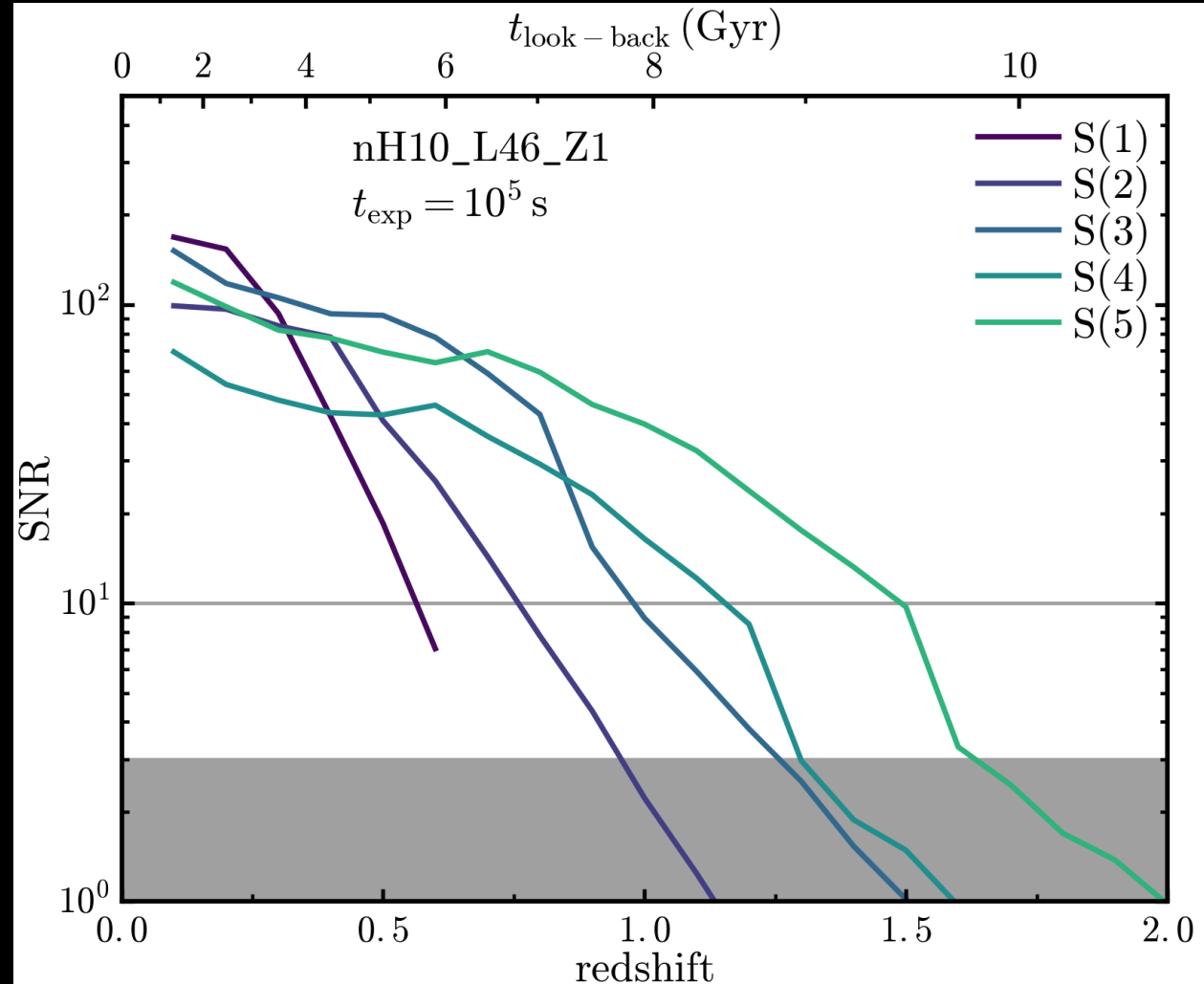
Richings & Faucher-Giguère (in prep)

# Warm H<sub>2</sub> Emission JWST Predictions



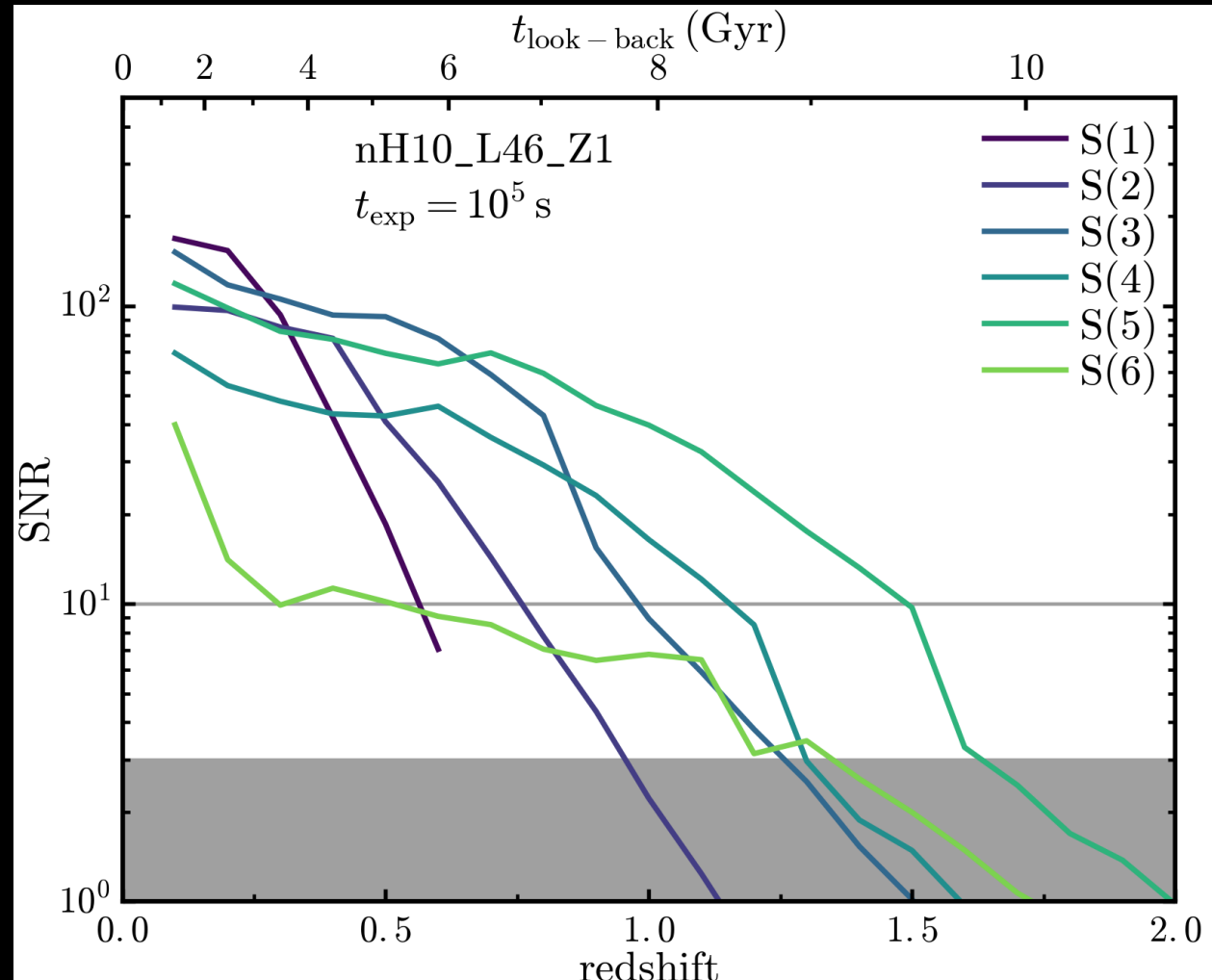
Richings & Faucher-Giguère (in prep)

# Warm H<sub>2</sub> Emission JWST Predictions



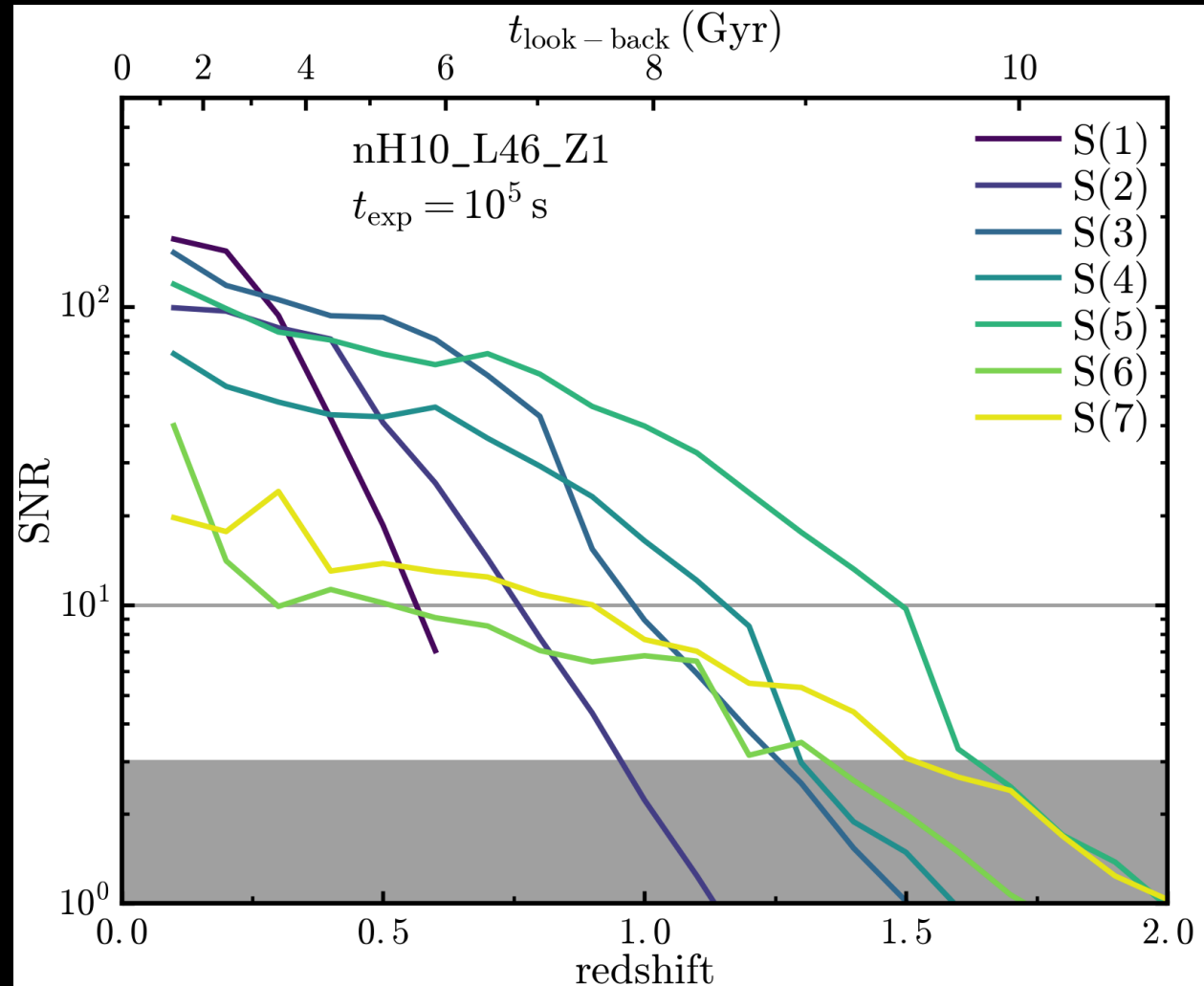
Richings & Faucher-Giguère (in prep)

# Warm H<sub>2</sub> Emission JWST Predictions



Richings & Faucher-Giguère (in prep)

# Warm H<sub>2</sub> Emission JWST Predictions



Richings & Faucher-Giguère (in prep)

# Summary

- Molecular outflow rates up to  $140 \text{ M}_{\text{sol}} \text{ yr}^{-1}$  formed within the AGN wind after 1 Myr.
- CO to H<sub>2</sub> conversion factor at solar metallicity:  
 $\alpha_{\text{CO(1-0)}} = 0.13 \text{ M}_{\text{sol}} (\text{K km s}^{-1} \text{ pc}^2)^{-1}$ .
- Strong warm H<sub>2</sub> emission, with  $T_{\text{exc}} \sim 400 \text{ K}$  at solar metallicity.
- Warm H<sub>2</sub> emission observable by JWST out to redshift 1.6 at an SNR of 3 (redshift 1.5 at an SNR of 10).